22.5°. Tapered fins, with a gap separation of 0.6 mm in the waveguide, were used to make radiation pattern measurements at 75 GHz. E- and H-plane radiation patterns of these measurements are shown in Figs. 5 and 6, along with calculated patterns. We conclude from these figures that the radiation patterns get narrower for the horn with the big flare angle, which corresponds to a big aperture area. We can also see that the patterns measured at 94 GHz are narrower than the ones measured at 75 GHz, which is expected since the electrical dimensions of the aperture become relatively large compared to the wavelength at higher frequencies. From our measurements of the radiation patterns of the finned structure at 94 GHz, we concluded that using the fins lowered the cutoff frequency of the waveguide without any significant effect on the radiation patterns. The comparison between the measured and calculated patterns shows, in general, a good agreement.

VI. Conclusions

W-band micromachined waveguides and horn antennas were fabricated using EDP anisotropic etching of silicon. Measurements of the dispersion curves were taken for finned waveguides with different fin separations. These measurements were compared to those calculated using the FEM technique, and the comparison showed a good agreement with an error in cutoff frequency of less than 3%. Radiation pattern measurements of horns were taken at 94 GHz before using the fins, then at 75 and 94 GHz after using fins in the structure to lower the cutoff frequency of the waveguide. Comparison between the measured and calculated patterns showed a good agreement. The fin structure can be transitioned into the coplanar waveguide for integration with monolithic system components.

Acknowledgment

The authors wish to express their gratitude to Dr. Yong Guo, TRW Inc., Redondo Beach, CA, for his collaboration in the formative stages of this paper.

References

[1] G. M. Rebeiz, D. P. Kasilingam, Y. Guo, P. A. Stimson, and D. B. Rutledge, "Monolithic millimeter-wave two-dimensional horn imaging arrays," *IEEE Trans. Antennas Propagat.*, vol. 38, pp. 1473–1482, Sept. 1990.

[2] Y. Guo, "Millimeter-wave integrated-circuit horn-antenna imaging arrays," Ph.D. dissertation, Dept. Elect. Eng., California Inst. Technol., Pasadena, CA, 1991.

[3] M. Yap, Y. Tai, W. R. McGrath, and C. Walker, "Silicon micromachined waveguides for millimeter and submillimeter wavelengths," in *Proc. IEEE 3rd Int. Space Terahertz Technol. Symp.*, Ann Arbor, MI, Mar. 1992, pp. 316–323.

[4] J. K. Johansson and N. D. Whyborn, "The diagonal horn as a sub-millimeter wave antenna," *IEEE Trans. Microwave Theory Tech.*, vol. 40, pp. 795–800, May 1992.

[5] B. Shenouda, L. W. Pearson, J. E. Harriss, W. Wang, and Y. Guo, "Etched-silicon micromachined waveguides and horn antennas at 94 GHz," in *IEEE AP-S Int. Symp. Dig* , Baltimore, MD, 1996, pp. 988–991.

[6] T. W. Crowe, P. J. Koh, W. L. Bishop, C. M. Mann, J. L. Hesler, R. M. Weikle, P. A. D. Wood, and D. Matheson, "Inexpensive receiver components for millimeter and submillimeter wavelengths," in *Proc. IEEE 8th Int. Space Terahertz Technol. Symp.*, Cambridge, MA, Mar. 1997, pp. 377–384.

[7] T. W. Crowe, J. L. Hesler, R. M. Weikle, and S. H. Jones, "GaAs devices and circuits for terahertz applications," *Infrared Phys. Technol.*, vol. 40, pp. 175–189, 1999.

[8] X. Wu, Q. Wu, and W. H. Ko, "A study on deep etching of silicon using ethylene–diamine–pyrocatechol–water," *Sens. Actuators*, vol. 9, pp. 333–343, 1986.

Improved Design of Broad-Band Latching Ferrite Phase Shifter in a Reduced-Size Grooved Waveguide

Wenquan Che, Edward Kai-Ning Yung, Wen Junding, and Kan Sha

***Abstract*—In this paper, an improved design of a broad-band latching ferrite phase shifter in grooved waveguide is discussed. The elimination technique for the insertion-loss peak is also introduced. The little gaps between the metal bars and waveguide wall are beneficial to suppress the high-order modes caused by the filling of high constant dielectric in the ferrite toroid. The theoretical and measured results have shown that the changes in differential phase shift with frequency remains less than 2.2%; the insertion loss and voltage standing-wave ratio of the device are good over the band 2∼4 GHz.**

***Index Terms*—Broad-band phase shifter, ferrite, grooved waveguide.**

I. Introduction

The development of a phased-array electronic-warfare system requires that the ferrite phase shifters have improved performance, such as shorter switch time, higher figure-of-merit, higher power-handling capacity, as well as broader bandwidth. Though the fluctuation of insertion loss and voltage standing-wave ratio (VSWR) for broad-band ferrite phase shifters are not critical in the system, many problems have existed in the design of the broad-band ferrite phase shifter [1], [2]. For example, there have been severe fluctuations of the insertion loss and a big slope of phase shift with frequency. In this paper, we present an improved design of the broad-band latching ferrite phase shifter in reduced-size grooved waveguide. Suitable selection of geometrical dimension and ridge height can result in smoother differential phase shift versus frequency; the little gaps existed in the innovative grooved waveguide are beneficial to suppress the high-order modes, which caused high loss peak. Furthermore, the coaxial-waveguide impedance-matching structure filled with dielectric can help to obtain good VSWR characteristic over the broad band. The experimental and theoretical results all show that, compared with the broad-band ferrite phase shifter in rectangular waveguide, the insertion loss of the ferrite phase shifter in grooved waveguide is decreased by 10%∼20%, differential phase shift is increased by 20%∼30%, the peak power capacity is improved by 10%, and the average power capacity is improved by 40%∼50%.

II. Design Considerations

A. Consideration of Differential Phase Shift Versus Frequency

1) Choice of Waveguide Structure: As we all know, the advantages of the ferrite phase shifter in grooved waveguide [3]–[6] are large differential phase shift, small insertion loss, and high power-handling capacity. However, there has been no literature on the broad-band ferrite phase shifter in grooved waveguide because the slope of the differen-

Manuscript received December 21, 1999; revised May 15, 2000. This work was supported by the Competitive Earmarked Research Grant, Research Grant Council, Hong Kong Special Administrative Region.

W. Che is with the Department of Electronic Engineering, City University of Hong Kong, Kowloon, Hong Kong and is also with the Department of Electrical Engineering, Nanjing University of Science and Technology, 210094 Nanjing, China.

E. K.-N. Yung is with the Department of Electronic Engineering, City University of Hong Kong, Kowloon, Hong Kong.

W. Junding and K. Sha are with the Department of Electrical Engineering, Nanjing University of Science and Technology, 210094 Nanjing, China.

Publisher Item Identifier S 0018-9480(01)02424-3.

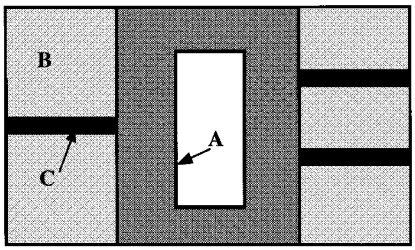

Fig. 1. Restraining technique for the higher modes of the ferrite phase shifter in rectangular waveguide. A: ferrite toroid. B: foam used to support the resistance sheet. C: resistance sheet.

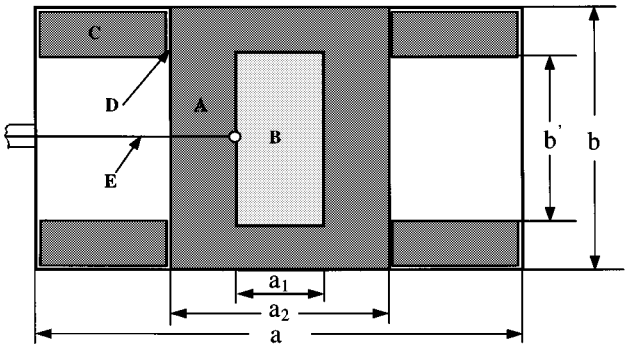

Fig. 2. Improved geometry of the broad-band latching ferrite phase shifter. A: ferrite toroid ($\varepsilon_{\mathrm{rf}} = 16.0$). B: loading dielectric ($\varepsilon_r = 32.0$). C: Metal bars. D: Little gap. E: switching wire $a = 22.85$, $b'/b = 0.625$, $a_1 = 3.0$, $a_2 = 10.0$, $4\pi Ms = 700$ Gs, $R = 0.75$.

tial phase shift versus frequency depends on the width of the waveguide and ridge height significantly. Based on the calculation, we choose the cross section of the grooved waveguide 22.86 mm × 10.16 mm, ridge height ratio $b'/b = 10/16$, reduced from the original rectangular waveguide whose cross-sectional dimension being 72.04 mm × 34.0 mm. Furthermore, a dielectric with a high dielectric constant ($\varepsilon_r = 32.0$) fills the ferrite toroid, which increases the differential phase shift significantly.

2) Choice of the Ridge Height: Due to its excellent performance, the latching ferrite phase shifter in grooved waveguide, which first appeared in the 1970's [3], has seen its wide application. The experiments have proven that, when $b'/b = 0.5$, the insertion loss is nearly two times of that when $b'/b = 0.625$. Field distribution analysis using a tensor finite-element method [7] indicates that there exists serious deformation of the electric field when $b'/b \leq 0.5$. Thus, we choose the ridge height ratio $b'/b = 0.625$. The measured results show that the figure-of-merit of the device has been improved significantly.

B. Consideration of Elimination Technique of Higher Order Modes

The theoretical results of the insertion loss calculated according to the formula in [3], [4], and [6] show that, over a broad band, the insertion loss versus frequency is relatively smooth. However, the measured insertion loss has indicated that there exists one high wide-band loss peak, which is very difficult to eliminate with normal ways. Actually, earlier in 1960's, a loss peak problem in the ferrite phase shifter in which a dielectric with a high dielectric constant was filled was reported [8]. It is obvious the nonuniformity and nonsymmetry of the ferrite phase shifter caused by the loading dielectric have excited some higher modes. We have made the following experimental studies.

1) We put the resistance sheets besides the two side of the ferrite toroid [9]. The geometry is illustrated in Fig. 1. The resistance sheets are parallel to the magnetic-field plane of the dominant mode; the loss peak cannot be removed. Actually, the position of insertion loss peak of LSE and LSM modes depends on the electrical length of the ferrite toroid. To realize good impedance matching, a dielectric toroid with the same dielectric constant as ferrite, which is also filled with dielectric ($\varepsilon_r = 32.0$) in the toroid, is cascade connected with ferrite toroid. It is found that the position of the loss peak has not changed. It indicates that the high order mode is not LSE_{11}, LSE_{12}, or LSE_{11} mode, and it is not a transmitting mode.
2) We changed the propagation direction of the microwave signal; the loss peak remained still. Believing that the loss peak is resulted from the TEM mode being resonant in the switching line, we took it out and the loss peak was still there. Obviously, it is not due to TEM mode coupling.
3) When another dielectric ($\varepsilon_r = 16.0$) was filled in the ferrite toroid, the insertion loss peak did not appear. Based on the preceding study, it is believed that the high constant dielectric loading ($\varepsilon_r = 32.0$) has excited evanescent waves in the ferrite phase shifter, which resulted in the high loss peak. Instead of the original ridge waveguide, four metal bars are put in the rectangular waveguide wall with screws, as shown in Fig. 2. Obviously, the waveguide is not a strict grooved waveguide, but it is equivalent to it. From the measured results shown in Fig. 3, we can see that the loss peak has disappeared. Clearly, the little gaps between the metal bars and waveguide wall have cut off the current of the high order modes caused by the filling of high constant dielectric in the ferrite toroid.

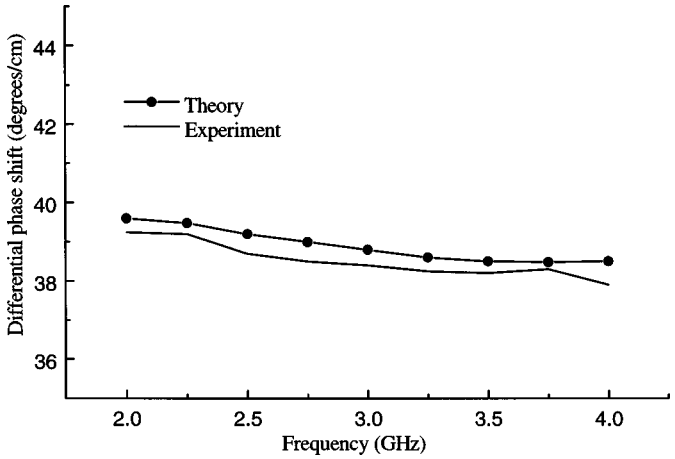

Fig. 3. Differential phase shifts versus frequency of the broad-band device.

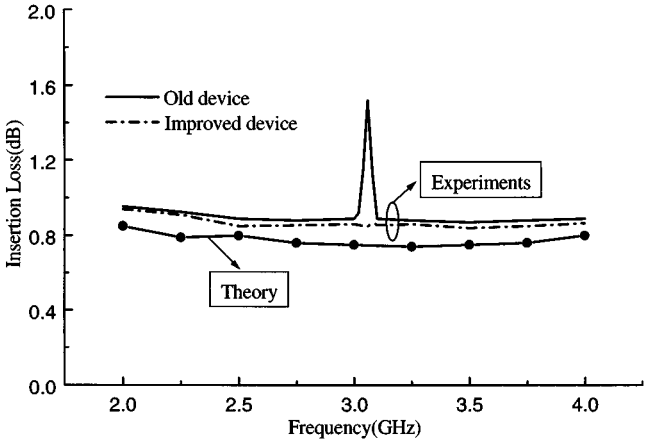

Fig. 4. Insertion losses versus frequency of the broad-band device.

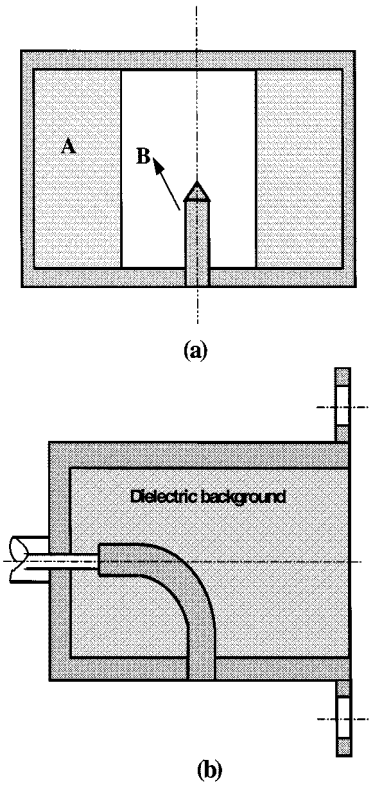

Fig. 5. Waveguide-coaxial impedance transformer in the broad-band device (a) Cross section. (b) Longitudinal section. A: dielectric ($\varepsilon_r = 16.0$). B: inner conductor of the axial line.

Thus, the insertion loss versus frequency of the device is considerably smoother.

III. Broad-Band Impedance-Matching Technique

The broad-band ferrite phase shifter utilizes reduced-size grooved waveguide. If the Chebyshev step impedance transformer is adopted to realize the broad-band characteristics of the ferrite phase shifter, it will enlarge the volume of the device greatly. Instead, we select a waveguide-coaxial impedance transformer loaded with dielectric ($\varepsilon_r = 16.0$). The experimental result indicates that the VSWR characteristic of the device (including transformer) is good over the broad band 2.0 GHz $\sim$ 4.0 GHz.

IV. Results and Discussion

A. Smooth Differential Phase Shift Versus Frequency

The experimental and theoretical studies all show that, if the width of the waveguide is too large, the slope of the differential phase shift versus frequency is positive, while if the width of the waveguide is too small, the slope is negative. Considering the slope of the phase shift versus frequency and the insertion loss, etc., the geometrical dimensions are decided and given in Fig. 2. The theoretical results of the differential phase shift calculated from the phase constant transcend [3, eq. (1)] together with the experimental results are plotted in Fig. 3. They indicate that the change of differential phase shift with frequency is less than 2.2% in the whole band ($f = 2.0$ GHz $\sim$ 4.0 GHz).

B. Insertion Loss

In order to increase the phase shift to some extent and not change the insertion loss significantly, instead of increasing the length of the ferrite, the ferrite toroid is filled with a high dielectric-constant material.

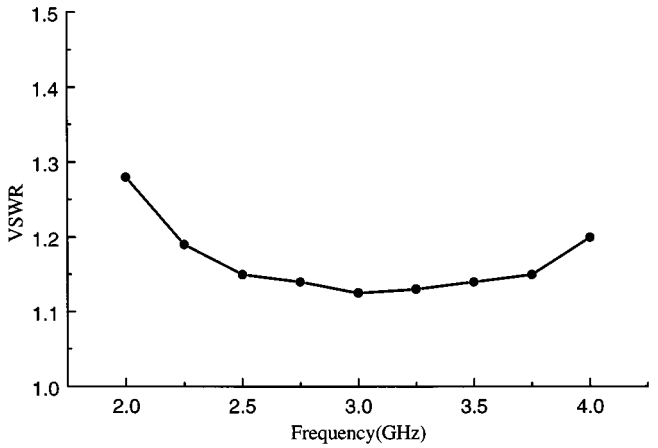

Fig. 6. Measured VSWR of the broad-band device.

The measured and theoretical results indicate that the differential phase shift is improved by 20%$\sim$30%. However, there existed a high insertion-loss peak, which is depicted as Fig. 4. At about $f = 3.05$ GHz, the insertion loss is as high as 1.5 dB. After an extended study, four metal bars are put in the rectangular waveguide to replace the traditional grooved waveguide. It is very fortunate that the high insertion-loss peak disappeared. The insertion loss versus frequency, also shown in Fig. 4, is relatively smooth. Clearly, the little gaps between the waveguide wall and ridges (i.e., metal bars) cut off the currents of the higher order modes, and thus they cannot be excited.

C. Wide-Band Characteristic in Terms of VSWR

In order to achieve wide-band VSWR characteristics, the waveguide-coaxial impedance transformer is adopted. Furthermore, the dielectric with the same dielectric constant as that of the ferrite toroid fills the waveguide, which is plotted in Fig. 5. It is very clear this kind of structure is in favor of reducing the difficulty of impedance matching. The measured result depicted in Fig. 6 shows that the VSWR characteristic of the phase shifter is good over the wide band. In the band 2$\sim$4 GHz, $\rho \leq 1.3$.

V. Conclusion

Improved design of the broad-band latching ferrite phase shifter in reduced-size grooved waveguide has been presented in this paper. An effective technique to eliminate the high loss peak has also been introduced here. The elimination of the higher order modes is due to the gaps between the metal bars and waveguide wall. Over the wide 2$\sim$4 GHz band, the insertion loss is relatively low, VSWR characteristics are good, and the change of the differential phase shift with frequency is less than 2.2%. The theoretical and measured results indicate that if we select a suitable design scheme, it is possible to manufacture high-quality broad-band ferrite phase shifters with higher figure-of-merit, bigger power-handling capacity, and smaller volume. These address the critical needs of the phased-array antenna of an electric–warfare system.

References

[1] H. Querido *et al.*, "Wide-band phase shifter," *IEEE Trans. Antennas Propagat.*, vol. AP-15, p. 300, Feb. 1967.
[2] E. -B. El-Sharawy and C. J. Koza, "Dual-ferrite slot line for broad-band, high-nonreciprocity phase shifters," *IEEE Trans. Microwave Theory Tech.*, vol. 39, pp. 2204–2210, Dec. 1991.
[3] W. Junding, "Analysis on the latching ferrite phase shifter in grooved waveguide," presented at the Nat. Magnet Mater. Device Conf., Sichuan, China, Oct. 1977.

[4] A. Mizobuchi and W. Kurebagashi, "Nonreciprocal remanance ferrite phase shifters using grooved waveguide," *IEEE Trans. Microwave Theory Tech.*, vol. MTT-26, pp. 1012–1017, Dec. 1978.
[5] W. Junding, Y. Z. Xiong, M. J. Shi, G. F. Cheng, and M. D. Yu, "Analysis of twin ferrite phase shifter in grooved waveguide," *IEEE Trans. Microwave Theory Tech.*, vol. 42, pp. 616–621, Apr. 1994.
[6] Y. S. Xu, "Microwave ferrite toroidal phase shifter in grooved waveguide with reduced sizes," *IEEE Trans. Microwave Theory Tech.*, vol. 36, pp. 1095–1097, June 1988.
[7] S. Chen, "Analysis of latching ferrite phase shifter in grooved waveguide using finite element methods," Masters thesis, Dept. Elect. Eng., Nanjing Univ. Sci. Technol., Nanjing, China, 1998.
[8] W. J. Ince *et al.*, "The use of manganese-doped iron garnets and high dielectric constant loading for microwave latching ferrite phasers," in *IEEE MTT-S Int. Microwave Symp. Dig.*, 1970, pp. 327–331.
[9] G. N. Tsandoula and D. H. Temmae *et al.*, "Longitudinal section mode analysis of dielectrically loaded rectangular waveguide with application to phase shifter design," *IEEE Trans. Microwave Theory Tech.*, vol. MTT-18, pp. 88–95, Feb. 1970.

A General Approach to Edge Singularity Extraction Near Composed Wedges in Boundary-Element Method

Pierluigi Cecchini, Fernando Bardati, and Rodolfo Ravanelli

***Abstract*—A general approach, based on the two-dimensional boundary-element method (BEM), has been proposed to extract the electromagnetic-field singularities in the presence of composed wedges, i.e., those formed by adjacent dielectric and conducting bodies. The method requires the knowledge of the field singularity order and is based on solution factorization into both a regular part and a singular one. Only the regular part has to be determined after extraction. No restrictions are imposed on position and order of singularities since each edge is treated independently of the others. Moreover, the method does not require the solution of further equations or use of special basis functions. It naturally extends the conventional BEM approach, improving its accuracy and convergence performances. Examples are given for a microstrip transmission line with a strip of finite thickness. The results show practicability and advantages of the new approach.**

***Index Terms*—BEM, edge singularity.**

I. Introduction

The electromagnetic-field behavior near composed wedges, formed by adjacent dielectric and conducting bodies, has been widely investigated by several authors. Adjacent wedges of different dielectric materials, as well as a conducting one, having the tip in common, compose the angular domain. Static solutions for this problem can be found in [1]–[6]. Meixner investigated the time-varying case [1] and postulated that the field near an edge can be locally expressed as a series, whose first term takes the singular behavior into account. In his analysis, the results for the static case are presented as the zero-frequency limit of the dynamic one. The static solution characterizes the local field behavior even in a time-varying case, which can be imagined as the quasi-static limit in a region whose dimensions, compared with the wavelength, are small. Andersen and Solodukhiov observed that the Meixner series is not self-consistent in the case where all wedges are dielectric and their angles are a fractional multiple of π [2]; the singularity order is still determined by the dominant static term. In [3], a characteristic equation was obtained for the singularity order in the general case of N dielectric wedges and a perfectly conducting one.

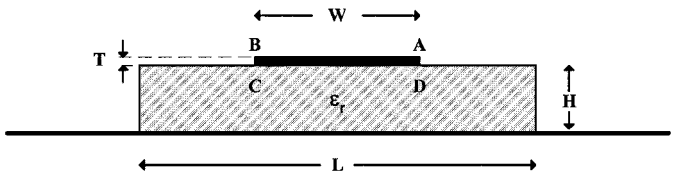

Fig. 1. Cross section of microstrip transmission line with truncated dielectric and finite thickness strip ($W = 4$ mm, $H = 2$ mm, $L = 24$ mm, $T = 0.2$ mm, $\varepsilon_r = 5$).

It is well known that the field singularities can be modeled for numerical computations in order to speed up convergence and reduce memory. In fact, direct numerical solutions to such problems require large numbers of basis functions and well-refined domain discretization [7], [8]. Alternatively, solutions can be achieved incorporating suitable edge-expansion functions into the numerical schemes [5], [9]–[13]. In problems that can be modeled by an integral equation over the interval $[-L, L]$, the edge condition can be expressed by means of a suitable entire-domain expansion

$$F(x) = \frac{1}{\left[1 - (x/L)^2\right]^{\alpha}} \sum_{n=0}^{\infty} c_n P_n^{\alpha}\left(\frac{x}{L}\right)$$

where $F(x)$ represents a singular field component, $\alpha \in (0, 1)$ is the order of the singularity as a function of the distance ρ from the tip (i.e., the field behaves as $1/\rho^{\alpha}$), and $P_n^{\alpha}(x/L)$ are orthogonal polynomials over $[-L, L]$ with respect to the weighting function $[1 - (x/L)^2]^{\alpha}$, such as Chebyshev $(\alpha = 0.5)$ or Gegenbauer polynomials. This approach properly works when the unknown function exhibits a symmetrical singular behavior at the end points of the interval.

On the other hand, sub-domain edge functions can only be used near edges, with the advantage that each edge can be treated in a different way. However, additional work may be necessary to implement different kinds of basis functions over each sub-domain and to link the solutions [5], [14]. A further technique, based upon the boundary integral equation [9], consists in approximating the field near an edge by the first N terms of the Meixner series, with unknown coefficients. The resulting linear problem has more unknowns than equations and further approximate conditions ($N - 1$ per edge) have to be imposed at suitable points away from the edge. In [9], an indirect BEM approach to handle square-root edge singularities has been presented with reference to microstrips. It is based on the extraction of factor $\sqrt{1 - (2x/w)^2}$ from the charge density over the strip (of width w) and leads to a linear system involving the remaining regular charge density factor.

In this paper, we generalize the last approach, developing a technique, suitable for BEM, to extract the field singularities, whose order has already been determined in the proximity of composed wedges. The method is able to solve problems with singularities of general order and position; it does not require the solution of additional equations and makes use of the same polynomial basis for both the composed wedge and regular boundary. Therefore, the present procedure can be easily implemented as an extension of a standard BEM code. It can

Manuscript received April 10, 2000.
P. Cecchini and F. Bardati are with the Dipartimento di Informatica, Universita Roma Tor Vegata, 00133 Rome, Italy.
R. Ravanelli is with the Alenia Aerospazio, 00131 Rome, Italy.
Publisher Item Identifier S 0018-9480(01)02426-7.